Original Article

Associations of osteoclastogenesis and nerve growth in subchondral bone marrow lesions with clinical symptoms in knee osteoarthritis

Feng Zhou [a,b,1], Xuequan Han [a,c,1], Liao Wang [a,1], Weituo Zhang [d], Junqi Cui [e], Zihao He [a], Kai Xie [a], Xu Jiang [a], Jingke Du [a], Songtao Ai [f], Qi Sun [f], Haishan Wu [a], Zhifeng Yu [a,*], Mengning Yan [a,**]

[a] *Shanghai Key Laboratory of Orthopaedic Implants, Department of Orthopaedic Surgery, Shanghai Ninth People's Hospital, Shanghai Jiao Tong University School of Medicine, Shanghai, China*
[b] *Department of Orthopaedic Surgery, The First Affiliated Hospital of Soochow University, Suzhou, Jiangsu, China*
[c] *Department of Orthopaedics, Qilu Hospital, Shandong University, Shandong University Center for Orthopaedics, Shandong University, Jinan, China*
[d] *Clinical Research Center, School of Medicine, Shanghai Jiao Tong University, Shanghai, China*
[e] *Department of Pathology, Shanghai Ninth People's Hospital, Shanghai Jiao Tong University School of Medicine, Shanghai, China*
[f] *Department of Radiology, Shanghai Ninth People's Hospital, Shanghai Jiao Tong University School of Medicine, Shanghai, China*

ABSTRACT

Background/objective: Subchondral bone marrow lesions (BMLs) are common magnetic resonance imaging (MRI) features in joints affected by osteoarthritis (OA), however, their clinical impacts and mechanisms remain controversial. Thus, we aimed to investigate subchondral BMLs in knee OA patients who underwent total knee arthroplasty (TKA), then evaluate the associations of osteoclastogenesis and nerve growth in subchondral BMLs with clinical symptoms.
Methods: Total 70 patients with primary symptomatic knee OA were involved, then separated into three groups based on MRI (without BMLs group, n = 14; BMLs without cyst group, n = 37; BMLs with cyst group, n = 19). Volume of BMLs and cyst-like lesions was calculated via the OsiriX system. The Western Ontario and McMaster Universities Osteoarthritis Index (WOMAC) questionnaire was used to assess clinical symptoms. Histology and immunohistochemistry were deployed to assess subchondral osteoclastogenesis and nerve distribution. Pearson's correlation coefficient was used to evaluate the associations between volume of BMLs and joint symptoms, and to assess the associations of osteoclastogenesis and nerve growth in subchondral BMLs with joint symptoms.
Results: In BMLs combined with cyst group, patients exhibited increased osteoclastogenesis and nerve distribution in subchondral bone, as shown by increased expression of tartrate resistant acid phosphatase (TRAP) and protein gene product 9.5 (PGP9.5). Volume of subchondral cyst-like component was associated with joint pain (p < 0.05). Subchondral osteoclastogenesis and nerve distribution were positively associated with joint pain in BMLs with cyst group (p < 0.05).
Conclusion: The subchondral cyst-like lesion was an independent factor for inducing pain in OA patients; osteoclastogenesis and nerve growth in subchondral cyst-like lesions could account for this joint pain.
The translational potential of this article: Our results indicated that the increased osteoclastogenesis and nerve growth in subchondral cyst-like lesions could account for the pain of OA joints. These findings may provide valuable basis for the treatment of OA.

1. Introduction

As a highly prevalent disorder of the musculoskeletal system, osteoarthritis (OA) is mainly characterized by joint pain, which greatly affects the quality of life [1]. In addition to pain, OA patients are susceptible to other clinical symptoms including joint stiffness and

---

functional disability [2].

Bone marrow lesions (BMLs) in subchondral bone are common pathological features during the progression of OA [3,4]. Basically, BMLs show a hyperintense signal in magnetic resonance imaging (MRI), similar to the edema-like signal. A specific proportion of BMLs exhibit well-defined regions of rounded hyperintense signals in MRI, commonly described as cyst-like lesions [5]. Although the underlying mechanism of subchondral bone cyst remains unclear, there are several existing theories including synovial fluid influx, bone contusion, vascular ageing and endothelial dysfunction [6].

Evidence has shown that BMLs in OA could up-regulate the expression of genes related to nerve growth, bone turnover, and inflammation [7]. Hence, subchondral BMLs have been demonstrated to be potentially associated with the clinical symptoms in OA patients [8]. In fact, studies have demonstrated that knee pain was associated with subchondral BMLs [9,10]. Moreover, the volume of subchondral cyst-like lesions was associated with knee pain [11]. However, the mechanism of pain in OA joints aroused from subchondral BMLs (including cyst-like lesions) remains unclear.

Osteoclastogenesis and nerve growth in subchondral bone were demonstrated to play important roles in causing pain of OA joints [12, 13]. Osteoclasts induce sensory nerve axonal growth via secreting netrin-1, while reduction of osteoclast formation in subchondral bone could inhibit the growth of sensory nerve and pain hypersensitivity in OA joints [12]. Moreover, osteoclasts are important sources of nerve growth factor (NGF), which could sensitize primary afferents in subchondral bone and lead to joint pain [13,14]. Therefore, we hypothesized that subchondral osteoclast densities might be increased in OA patients when combined with BMLs, and that the increased osteoclastogenesis could cause subchondral nerve growth, further arousing pain in OA joints.

In this study, we enrolled symptomatic knee OA patients who underwent total knee arthroplasty (TKA). We aimed to determine the association of osteoclastogenesis and nerve growth in subchondral BMLs (including the subtypes) with clinical symptoms in OA patients. By analyzing the relationships between histological parameters and clinical symptoms, we hoped to clarify how subchondral BMLs could cause joint pain in OA patients.

2. Materials and methods

2.1. Subjects

This cross-sectional study was approved by the Ethics Committee of Shanghai Ninth People's Hospital (NO. 2018-151-T137). All patients provided written informed consent. Participants involved were diagnosed with primary symptomatic knee OA based on clinical and radiographic criteria. Specifically, weightbearing anteroposterior radiographs of the knee joints were obtained, then the severity of OA was graded based on the Kellgren–Lawrence (K-L) classification system [15]. Patients involved in this study were in K-L grade III/IV. Those who had other forms of arthritis such as rheumatoid arthritis (RA), or who were taking medications that could affect bone remodeling (including estrogen and bisphosphonates) were excluded. Subjects underwent TKA in the Department of Orthopaedics Surgery, Shanghai Ninth People's Hospital. Total 70 patients were involved and divided into three groups based on MRI [11]. One group was without BMLs (n = 14, mean age 63.93 ± 9.65), one group had subchondral BMLs without cyst-like lesions (n = 37, mean age 65.14 ± 8.57), and the third group had subchondral BMLs with cyst-like lesions (n = 19, mean age 66.47 ± 9.81).

2.2. Assessment of OA clinical symptoms

The Western Ontario and McMaster Universities Osteoarthritis Index (WOMAC) questionnaire was deployed to assess pain, stiffness, and function of the OA knee joints. Briefly, in the Likert format, the subscale scores are: pain (0–20, 5 items), stiffness (0–8, 2 item), and physical function (0–68, 17 item); each item is scored on a 0–4 scale. In the visual analogue scale (VAS) format, the ranges for three subscale scores are: pain, 0–500; stiffness, 0–200; and physical function, 0–1700. WOMAC total score was the sum of pain, stiffness, and function score [16]. In this study, participants were required to associate their scores with clinical symptoms within the last 48 h for getting WOMAC score. Then, the WOMAC score was recorded in VAS format and normalized to 100 units.

2.3. MRI acquisition

The index knee joints were pre-operatively scanned with a MAGNE-TOM Skyra 3.0 T MRI system (Siemens, Germany), utilizing a dedicated phased-array knee coil. A proton density-weighted (PD) fat-suppressed (FS) fast spin echo (FSE) sequence was applied [17]. The parameters were as follows: sagittal, repetition time (TR) 4500 ms, echo time (TE) 34 ms, slice thickness 4 mm, slice gap 0.2 mm, acquisition matrix 288 × 192, and axial, TR 3600 ms, TE 22 ms, slice thickness 4 mm, slice gap 0.2 mm, and acquisition matrix 256 × 192.

2.4. MRI based quantitative assessment

BMLs were characterized as ill-defined hyperintense (edema-like) regions on PD FS MRI sequence. To verify the subchondral BMLs, the edema-like hyperintense signal must have been adjacent to the articular cartilage or the cartilage loss area on at least a single MRI slice [11]. BMLs were subdivided into two subtypes based on with or without cyst-like component. More specifically, BMLs combined with cyst-like components were defined as those in which the cyst-like components were seen in more than two adjacent slices in MRI images [11].

The volumetric calculation of BMLs was performed by an experienced radiologist via the OsiriX system (edition 10.0, PixMeo SARL) in a blinded manner. Briefly, BMLs in each subregion were manually marked on MRI. Then, 3D post-processing techniques in the OsiriX system were applied to calculate the volume of BMLs [18]. 3D slicer (edition 4.11.20200930) was used to reconstruct the structure of the knee joint, including subchondral BMLs. When calculating the total volume of BMLs, all subchondral BMLs with or without cyst-like components were included. The cyst-like component volume was calculated, excluding hyperintense signals within osteophytes and the cyst-like components without surrounding ill-defined hyperintense signal.

2.5. Sample processing

After TKA, mid-coronal regions of the middle third of the medial tibial plateau, which were important for weight-bearing, were segmented [13]. The samples were fixed with 4% paraformaldehyde for 48 h then rinsed overnight. The specimens were decalcified in 10% ethylenediaminetetraacetic acid (EDTA) in 10 mM Tromethamine (Tris) buffer for 28 days and then embedded with paraffin.

2.6. Histological observation

Samples were sliced at 5 μm and then processed with hematoxylin and eosin (H&E) and safranin O/fast green (S&F) staining. The Osteoarthritis Research Society International (OARSI) score which can reflect cartilage damage was calculated as described previously [19]. Briefly, the OARSI scoring was based on six grades (0–6) reflecting lesion depth and four stages (0–4) reflecting lesion extent. OARSI score = grade × stage, this method produces OA score with a range from 0 to 24. The OARSI score in this study was performed by two experienced observers in a blind way; there was no significant difference in the results obtained by the two observers.

2.7. Immunohistochemistry

Five sequential slides in each specimen were stained and evaluated.

Tartrate resistant acid phosphatase (TRAP) was chosen as a marker for osteoclasts, and protein gene product 9.5 (PGP9.5) as a marker for nerve [20,21]. Sections were first blocked with 5% bovine serum albumin (BSA), then incubated with anti-TRAP antibody (Abcam, mouse, dilution 1:200) for 12 h. After being washed with phosphate buffered saline (PBS) three times, samples were incubated with anti-PGP9.5 antibody (Sigma–Aldrich, rabbit, dilution 1:100) for another 12 h. Green (Abcam, Alexa Fluor® 488, donkey anti-mouse, 1:500) and red (Abcam, Alexa Fluor® 594, goat anti-rabbit, dilution 1:500) fluorescent secondary antibodies were in turn deployed for 1 h. Anti-matrix metalloprotein 13 (MMP-13) antibody (Abcam, mouse, dilution 1:200) was administrated for 12 h then stained with green fluorescent secondary antibody (Abcam, Alexa Fluor® 488, donkey anti-mouse, 1:500). Isotype controls including mouse IgG (Abcam, dilution 1:200) and rabbit IgG (Abcam, dilution 1:200) were applied to exclude the non-specific staining. Finally, the sections were stained with 4,6-diamidino-2-phenylindole (DAPI) for 15 min then photographed using a confocal fluorescence microscope (Leica, Germany). The red/green fluorescence represents positively stained cells, then number of positive cells per unit area was calculated.

2.8. Statistical analysis

The data were expressed as mean ± standard deviation and presented in a box–whisker plot. The top line of the box–whisker plot represents the maximum value, while the bottom line represents the minimum value. The upper margin of the box is the upper quartile, the middle line is the median, lower margin of the box is the lower quartile. The data were tested for normality by the Shapiro–Wilk test. The two-sided Student's t test was used to compare normally distributed clinical variables. Otherwise, the Kruskal–Wallis (K–W) test was utilized for analyzing non-normally distributed data. One-way analysis of variance (ANOVA) was applied to compare the variables in various groups. Variables were compared again after adjusting for each potential covariate by a multiple linear regression analysis. Covariates independent from each other were selected, including age, height, weight, body mass index (BMI) and K-L grade. Pearson's correlation coefficient was deployed to analyze the relationships between BMLs (including the subtypes) and OA symptoms. For all the analyses, a two-tailed $p < 0.05$ was regarded as statistically significant. All data analyses were conducted using the SPSS 22.0 statistical software package (SPSS Inc, Chicago, USA).

3. Results

Patients were divided into three groups based on BMLs and the combination of cyst-like lesions (Fig. 1a–c). 3D reconstructed images showed the location of BMLs with cyst in subchondral bone (Fig. 1d–f). Age, height, weight, and BMI in the three groups showed no significant differences ($p > 0.05$). In looking at clinical symptoms, patients in BMLs with cyst group demonstrated significant increased WOMAC pain score compared with patients in the other two groups ($p < 0.05$). Although the WOMAC stiffness and function scores were increased in BMLs with cyst group, they showed no significant differences compared with the other two groups ($p > 0.05$) (Table 1).

Pearson's correlation coefficient analysis showed that the volume of subchondral BMLs with or without cyst-like lesions demonstrated no significant association with WOMAC total, pain, stiffness, and function score ($p > 0.05$). Volume of the subchondral cyst-like component itself was significantly associated with WOMAC total, pain, and function score ($p < 0.05$), while it demonstrated no obvious association with WOMAC stiffness score ($p > 0.05$) (Table 2). These results suggested that the subchondral cyst itself was an important and independent factor for causing joint pain and functional disability.

Compared with patients without BMLs or with simple BMLs, patients with BMLs combined with cysts-like lesions exhibited necrotic bone fragments accompanied by surrounding fibrous connective tissue in H&E staining (Fig. 2a). Cartilage damage revealed by S&F staining
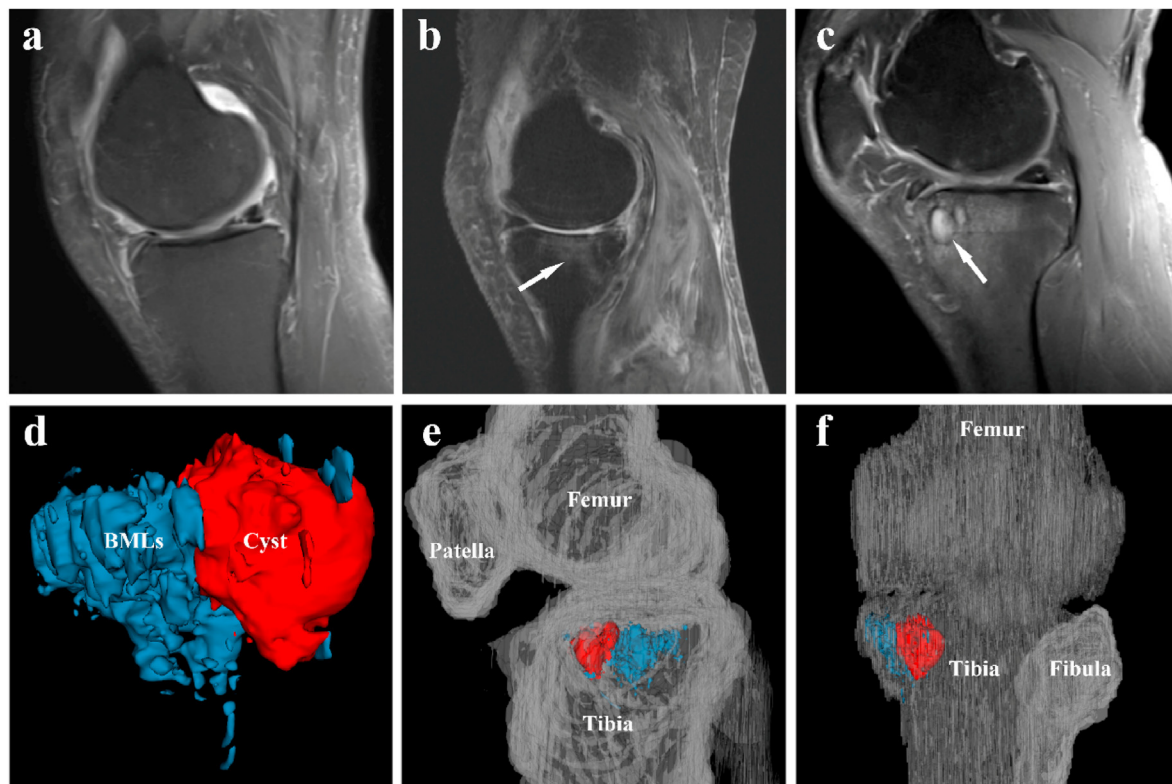
Figure 1. MRI images of various types of BMLs. (a) OA patient without BMLs. (b) Subchondral BMLs without cyst-like component (white arrows) in the tibia. (c) BMLs combined with cyst-like component (white arrows) in the tibia. (d) 3D image of subchondral BMLs combined with cyst (e, f) 3D models of the knee joint were reconstructed based on the MRI images.

Table 1
Patients and basic information.

Characteristics	Without BMLs (n = 14)	BMLs without cyst (n = 37)	BMLs with cyst (n = 19)
Age (years)	63.93 ± 9.65	65.14 ± 8.57	66.47 ± 9.81
Sex, n (male/female)	4/10	14/23	5/14
Height (cm)	164.36 ± 7.01	162.43 ± 7.52	160.58 ± 6.31
Weight (kg)	65.36 ± 5.67	66.46 ± 7.33	64.37 ± 8.33
Hypertension, n (%)	4 (28.57)	11 (29.73)	6 (31.58)
Diabetes, n (%)	2 (14.29)	7 (18.92)	3 (15.79)
BMI (kg/m^2)	24.25 ± 2.31	25.21 ± 2.55	24.97 ± 3.00
Index knee, n (right/left)	8/6	17/20	9/10
Kellgrene-Lawrence grade, n (grade III/IV)	7/7	22/15	13/6
WOMAC total score	35.33 ± 13.25	36.50 ± 8.35	40.37 ± 7.33
WOMAC pain score	30.29 ± 4.50	31.73 ± 6.17	36.63 ± 8.19**#
WOMAC stiffness score	43.57 ± 17.03	44.73 ± 13.69	46.05 ± 15.15
WOMAC function score	35.42 ± 19.17	36.93 ± 11.20	40.80 ± 8.18
Total BMLs volume (mm^3)	—	1794.15 ± 1815.47	1351.95 ± 808.50
Subchondral BMLs without cyst (mm^3)	—	1794.15 ± 1815.47	—
Subchondral BMLs with cyst (mm^3)	—	—	1351.95 ± 808.50
Volume of the cyst (mm^3)	—	—	152.48 ± 138.02

Symbol "*" indicates comparisons with the first group, "*" indicates p < 0.05, "**" indicates p < 0.01. Symbol "#" indicates comparisons with the second group, "#" p < 0.05, "##" indicates p < 0.01.

Table 2
Correlation coefficient between volume of BMLs and symptoms of OA.

| Group	WOMAC total score	WOMAC pain score	WOMAC stiffness score	WOMAC function score
BMLs (n = 56)	0.213	0.101	0.145	0.193
BMLs without cyst (n = 37)	0.290	0.156	0.201	0.252
BMLs with cyst (n = 19)	0.109	0.224	0.012	0.069
Cyst (n = 19)	0.713**	0.685**	0.148	0.668**

Symbol "*" indicates correlation between various types of BMLs and symptoms of OA, "*" indicates p < 0.05, "**" indicates p < 0.01.

demonstrated more severe damage in patients with BMLs combined with cyst-like lesions, as shown by increased destruction and decreased thickness of the articular cartilage (Fig. 2b). Comparison of OARSI score showed that there was no significant difference between the group without BMLs and the group with simple BMLs, while OARSI score was obviously increased in the group with BMLs combined with cyst-like lesions (p < 0.01) (Fig. 2c).

To examine the mechanism of joint pain caused by subchondral cyst-like lesions, we deployed TRAP and PGP9.5 double immunofluorescence staining to detect subchondral osteoclastogenesis and nerve distribution. Enhanced red and green fluorescence staining revealed that osteoclast density and nerve distribution were obviously increased in patients with BMLs combined with cyst-like lesions. Moreover, most of the red fluorescence (nerve fiber) was co-localized with green fluorescence (osteoclast), indicating that the subchondral nerve growth may have been induced by the osteoclasts (Fig. 3a). Quantitative analysis showed that the number of TRAP/PGP9.5 positive cells had no obvious difference between the group without BMLs and the group with simple BMLs (p > 0.05), however, it was significantly increased in the group with BMLs combined with cyst-like lesions (p < 0.01) (Fig. 3b and c).

We further detected the expression of MMP-13 which is a key factor for promoting osteoclast differentiation and activation in subchondral bone [22,23]. Similarly, subchondral MMP-13 expression was significantly increased in the BMLs with cyst-like lesions group (p < 0.01) (Fig. 4a and b). These results demonstrated that osteoclasts were increased in patients with BMLs accompanied with subchondral cyst-like lesions, which could account for the increased nerve growth in the subchondral bone.

We detected the association of clinical symptoms of OA with subchondral osteoclast density and nerve growth via Pearson's correlation coefficient. Results demonstrated that TRAP, PGP9.5, and MMP-13 expression were significantly associated with WOMAC total, pain, and function score in BMLs combined with cyst group (p < 0.05). As for the other two groups, subchondral TRAP, PGP9.5, and MMP-13 expression showed no statistically significant association with WOMAC total, pain, stiffness, and function score (p > 0.05) (Table 3). These results suggested that osteoclastogenesis and nerve growth in subchondral cysts might account for the pain and functional disability of OA joint.
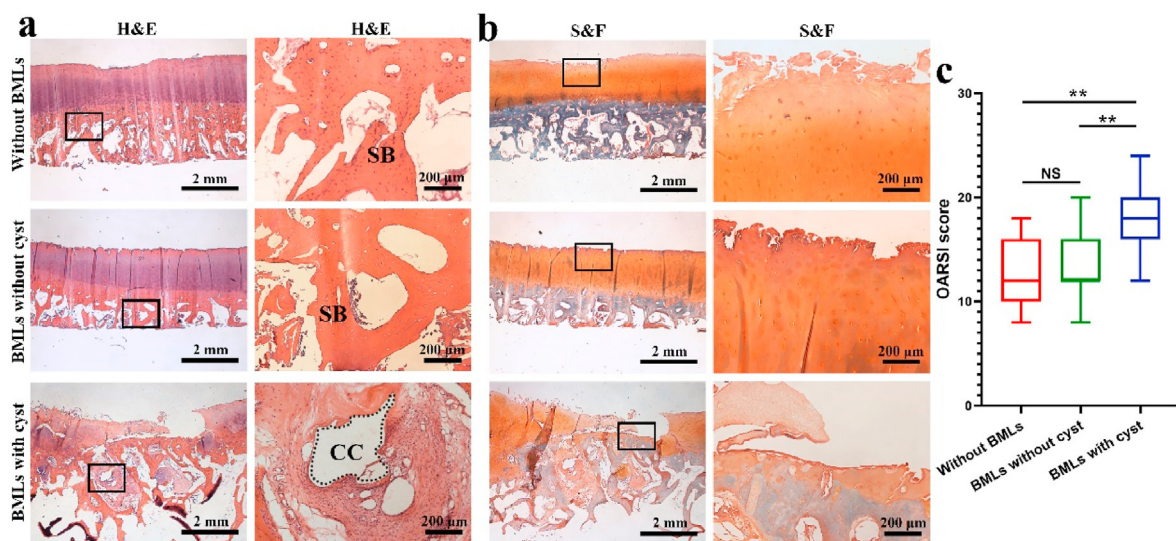
Figure 2. Histological observation of subchondral bone and articular cartilage. (a) H&E staining showed the structure of subchondral bone. (b) S&F indicated the cartilage damage among the three groups of patients. (c) OARSI score of the cartilage in the tibia, compared by K–W test. "*" indicated p < 0.05, "**" indicated p < 0.01, "CC" indicated cystic cavity, "SB" indicated subchondral bone.
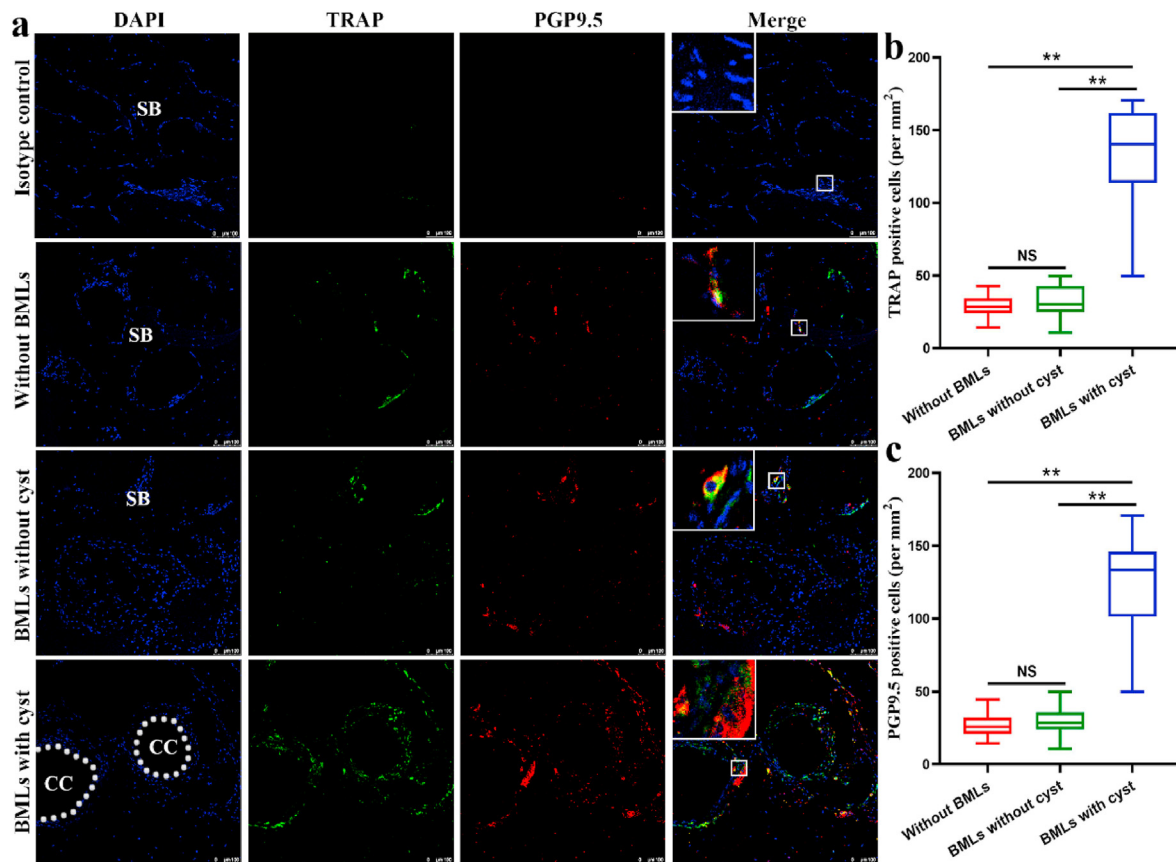
Figure 3. Osteoclast density and nerve growth in subchondral bone. (a) TRAP/PGP9.5 double immunofluorescence staining. (b) Quantitative analysis of TRAP among the three groups, compared by K–W test. (c) Quantitative analysis of PGP9.5 among the three groups, compared by Student's t test. "*" indicated p < 0.05, "**" indicated p < 0.01, "CC" indicated cystic cavity, "SB" indicated subchondral bone.

4. Discussion

BMLs have been shown as an important feature in OA, however, the relationship between BMLs and OA joint pain has remained controversial [24]. Two observational studies demonstrated that knee pain was associated with increased subchondral BMLs [9,10]. However, in a secondary study of a randomized trial, results showed that there was no significant association between the volume of BMLs and OA joint pain [11]. Our data were consistent with results of the later research, in that there was no significant correlation between subchondral total BMLs volumes and pain. The association between subchondral cyst-like lesions and pain was also an uncertainty. Two cross-sectional studies which used a semi-quantitative approach had proposed that subchondral cysts were not associated with symptoms of OA [25,26]. Nevertheless, another study indicated that increased subchondral cyst volume was associated with more severe knee pain [11]. We showed that knee pain and function was associated with volume of the cyst-like component. Different results in these studies may have been induced by differences in the populations, assessment methods, and type of MRI sequence.

Subchondral cyst-like lesions are a common phenomenon in knee patients with OA. However, the cause of cyst-like lesion formation remains unclear. The synovial fluid intrusion theory proposed that increased intra-articular pressure causes joint fluid to infiltrate into subchondral bone through the fissured or ulcerated cartilage, which then develops into a cyst [27]. Based on this theory, subchondral cysts should develop in the regions with existing cartilage loss or fissuring. Another theory, the bone contusion theory, put forward that a subchondral cyst was a consequence of a traumatic bone contusion [28]. In fact, a previous study demonstrated that subchondral cysts were commonly observed in areas of pre-existing BMLs [29]; this could support the bone contusion

theory. Pok Man Boris Chan et al. provided a new angle for understanding the pathophysiology of subchondral bone cysts. They proposed that subchondral cyst-like lesions especially in non-load-bearing region are results of vascular ageing and endothelial dysfunction. In particular, they proposed that ischemic episodes, endothelial senescence, insufficient H-type (CD31^{hi}, EMCN^{hi}) vessel, loss of pericyte and osteoprogenitors were associated with subchondral cysts [6].

Histologically, literature has revealed that most simple BMLs were subchondral bone with normal structure; only a small proportion demonstrated non-characteristic abnormalities such as bone marrow necrosis, bone marrow fibrosis and edema, and abnormal trabeculae [30]. However, the cyst-like lesions were usually composed of necrotic bone fragments and dead denuclearized cells. Moreover, the cystic cavities were demonstrated to be surrounded by fibrous connective tissue, which contained osteoblasts and adipocytes [31]. In this study, we found that the cyst-like lesions showed necrotic bone fragments which were surrounded by fibrous connective tissue. In addition, when BMLs were combined with a cyst, there was destruction of the subchondral structure. We also found that TRAP positively stained cells were increased mainly on the surface of cysts, indicating that osteoclasts were activated around the cysts. This might account for the formation of cyst-like lesions.

Subchondral bone has been demonstrated to be an important supporting structure for the upper cartilage, and disturbance of subchondral bone remodeling was closely related to the progression of OA [32,33]. A study has demonstrated that MMP-13, an important bone resorptive factor, was elevated in OA subchondral bone [17]. Other researches have supposed that subchondral MMP-13, mainly drived from osteoblasts, could work synergistically with cathepsin K and cause suchondral bone resorption [34]. Moreover, osteocytes were also deomonstrated to be an important source of MMP-13 [35]. MMP-13 could cause type I collagen
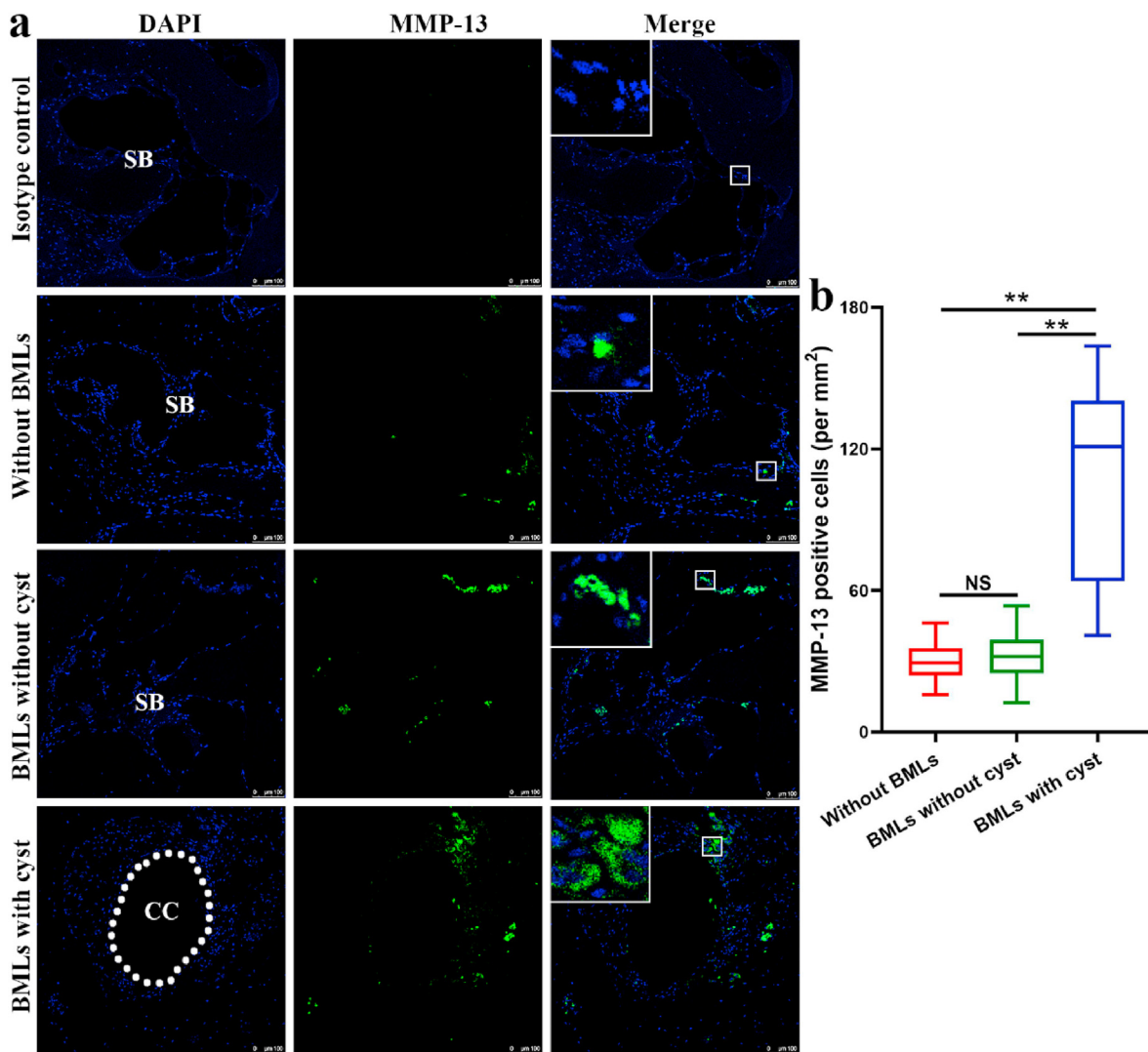
Figure 4. Expression of MMP-13 in subchondral bone. (a) MMP-13 immunofluorescence staining in subchondral bone. (b) Quantitative analysis of MMP-13 among the three groups, compared by K–W test. "*" indicated p < 0.05, "**" indicated p < 0.01, "CC" indicated cystic cavity, "SB" indicated subchondral bone.

Table 3
Correlation coefficient between subchondral osteoclast/nerve growth and symptoms in various groups.

Group	WOMAC score	TRAP	PGP9.5	MMP-13
Without BMLs	WOMAC total score	−0.335	0.068	−0.087
	WOMAC pain score	0.445	−0.158	0.155
	WOMAC stiffness score	−0.017	−0.023	0.382
	WOMAC function score	−0.360	0.051	−0.117
BMLs without cyst	WOMAC total score	−0.025	−0.126	0.234
	WOMAC pain score	0.240	0.183	0.305
	WOMAC stiffness score	0.052	0.271	0.124
	WOMAC function score	−0.072	−0.201	0.178
BMLs with cyst	WOMAC total score	0.850**	0.586**	0.726**
	WOMAC pain score	0.653**	0.520*	0.472*
	WOMAC stiffness score	0.367	0.053	0.151
	WOMAC function score	0.803**	0.577**	0.747**

Symbol "*" indicates correlation between subchondral osteoclast/nerve growth and clinical symptoms of OA, "*" indicates p < 0.05, "**" indicates p < 0.01.

degradation and contribute to osteoclast differentiation and the resultant increased bone resorption process [22,23]. In the present study, MMP-13 was found to be significantly increased in the subchondral bone of OA patients with BMLs combined with cyst-like lesions. Moreover, the cartilage damage was more serious in the BMLs with cyst-like lesion group. The increased expression of subchondral MMP-13 caused increased osteoclast density and resultant enhanced bone resorption, which may have accounted for the more severe cartilage damage.

Several subsets of immune cells are involved in subchondral BMLs in OA joints. Macrophage infiltration and osteoclast formation in the subchondral bone were characteristic pathological changes in subchondral BMLs in OA [3,36]. Macrophages (both M1 and M2 type) could stimulate angiogenes via releasing vascular endothelial growth factor (VEGF), causing lesions in subchondral bone [37]. On the other hand, it was demonstrated that M1 phenotype macrophages may be a transient state similar to pre-osteoclast, which could finally turn into osteoclasts [38]. Besides macrophages, lymphocytes including T cells and B cells were also demonstrated to infiltrate in subchondral bone of OA. T cells and B cells as the major effectors in the adaptive immunity are involved in osteoclastogenesis and bone erosion [39].

Osteoclasts can cause pain in OA joints via inducing nerve growth in subchondral bone. For one thing, osteoclasts could induce sensory nerve axonal growth via secreting netrin-1 and cause pain hypersensitivity in OA joints [12]. For another, osteoclasts were demonstrated to be an important source of NGF, which is capable of sensitizing subchondral primary afferents [13]. NGF may have accounted for the generation of joint pain, as it could directly activate sensory neurons by combining with tyrosine kinase A (TrkA) [40]. Moreover, the deployment of

anti-NGF antibodies could reduce pain of OA joints, demonstrating that NGF may be important for pain generation [41]. Increased subchondral NGF has been found to further induce nerve growth, which may arouse joint pain [14,42]. It has previously been indicated that subchondral multinucleate osteoclasts are co-localized with NGF [13], therefore we directly applied co-localization staining of osteoclasts and nerve fibers. Results showed that most of the nerve fibers (red fluorescent) were co-localized with osteoclasts (green fluorescent), indicating that subchondral osteoclasts may induce nerve growth. These results supported our hypothesis that osteoclasts were increased in OA patients with BMLs combined with cyst-like lesions, and the pain mechanism may be due to osteoclasts causing nerve growth in the subchondral bone.

Angiogenesis is an important pathological feature during the progression of OA. Platelet-derived growth factor-BB (PDGF-BB) secreted by preosteoclasts could induce H-type vessel formation, further affecting bone modeling and remodeling [43]. Moreover, angiogenesis and nerve growth are closely interacting processes. Vascular cells could induce nerve growth by producing several regulators of nerve growth [14]. Therefore, angiogenesis was supposed to contribute to pain in OA. However, pain as the most common symptom in OA patients is mediated by sensory nerve [44]. Thus, we paid more attention to nerve growth rather than angiogenesis in this study.

We must emphasize that osteoclasts may cause joint pain through multiple channels. Osteoclasts may directly change subchondral structure, hence affecting subchondral biochemical properties [45]. Osteoclasts may secrete angiogenic factors which lead to blood vessel formation in the subchondral bone, further contributing to the pain of OA [14,44]. Other factors besides osteoclasts could also account for joint pain. For example, osteocytes are potential players in OA pain, as they can produce NGF particularly in an inflammatory environment [46]. For another, synovitis has been proven to be a notable factor for causing OA joint pain [47]. In the present study, we focused on the pathology of BMLs and cyst-like lesions in subchondral bone. Therefore, we evaluated the changes of subchondral osteoclasts and the following nerve growth.

Some limitations of this study need to be considered. First, there are other types of BMLs such as ligament-based BMLs [11], while we focused on subchondral BMLs and cyst-like lesions as we wanted to explore how subchondral BMLs could cause joint pain. Moreover, subjects involved in this study were all symptomatic OA knee patients, we did not evaluate the subchondral osteoclastogenesis and nerve growth in asymptomatic patients with OA. Despite these limitations, our study is valuable in describing how subchondral cyst-like lesions could cause joint pain.

In conclusion, our study demonstrated the subchondral changes and increased cartilage damage in OA patients who had BMLs with cyst-like lesions. Moreover, the relationships between BMLs and clinical symptoms of OA indicated that the volume of cyst-like lesions was associated with pain in symptomatic OA knee patients. Furthermore, the increased subchondral osteoclastogenesis and nerve growth induced by the cyst-like lesions may have accounted for the pain of OA joints. Thus, our study supported the potential explanation for the mechanism of subchondral cyst-like lesions in causing joint pain.

Funding

Declaration of competing interest

The authors have no conflicts of interest to disclose in relation to this article.

Acknowledgements

References

[1] Wu X, Wang Y, Xiao Y, Crawford R, Mao X, Prasadam I. Extracellular vesicles: potential role in osteoarthritis regenerative medicine. J Orthop Translat 2020;21: 73–80.

[2] Huang W, Ong TY, Fu SC, Yung SH. Prevalence of patellofemoral joint osteoarthritis after anterior cruciate ligament injury and associated risk factors: a systematic review. J Orthop Translat 2020;22:14–25.

[3] Hügle T, Geurts J. What drives osteoarthritis?-synovial versus subchondral bone pathology. Rheumatology 2017;56(9):1461–71.

[4] Findlay DM, Kuliwaba JS. Bone-cartilage crosstalk: a conversation for understanding osteoarthritis. Bone Res 2016;4:16028.

[5] Crema MD, Roemer FW, Zhu Y, Marra MD, Niu J, Zhang Y, et al. Subchondral cystlike lesions develop longitudinally in areas of bone marrow edema-like lesions in patients with or at risk for knee osteoarthritis: detection with MR imaging–the MOST study. Radiology 2010;256(3):855–62.

[6] Chan PMB, Wen C, Yang WC, Yan C, Chiu K. Is subchondral bone cyst formation in non-load-bearing region of osteoarthritic knee a vascular problem? Med Hypotheses 2017;109:80–3.

[7] Kuttapitiya A, Assi L, Laing K, Hing C, Mitchell P, Whitley G, et al. Microarray analysis of bone marrow lesions in osteoarthritis demonstrates upregulation of genes implicated in osteochondral turnover, neurogenesis and inflammation. Ann Rheum Dis 2017;76(10):1764–73.

[8] Driban JB, Price L, Lo GH, Pang J, Hunter DJ, Miller E, et al. Evaluation of bone marrow lesion volume as a knee osteoarthritis biomarker–longitudinal relationships with pain and structural changes: data from the Osteoarthritis Initiative. Arthritis Res Ther 2013;15(5):R112.

[9] Lo GH, McAlindon TE, Niu J, Zhang Y, Beals C, Dabrowski C, et al. Bone marrow lesions and joint effusion are strongly and independently associated with weight-bearing pain in knee osteoarthritis: data from the osteoarthritis initiative. Osteoarthritis Cartilage 2009;17(12):1562–9.

[10] Felson DT, Niu J, Guermazi A, Roemer F, Aliabadi P, Clancy M, et al. Correlation of the development of knee pain with enlarging bone marrow lesions on magnetic resonance imaging. Arthritis Rheum 2007;56(9):2986–92.

[11] Perry TA, Parkes MJ, Hodgson RJ, Felson DT, Arden NK, O'Neill TW. Association between Bone marrow lesions & synovitis and symptoms in symptomatic knee osteoarthritis. Osteoarthritis Cartilage 2020;28(3):316–23.

[12] Zhu S, Zhu J, Zhen G, Hu Y, An S, Li Y, et al. Subchondral bone osteoclasts induce sensory innervation and osteoarthritis pain. J Clin Invest 2019;129(3):1076–93.

[13] Aso K, Shahtaheri SM, Hill R, Wilson D, McWilliams DF, Walsh DA. Associations of symptomatic knee osteoarthritis with histopathologic features in subchondral bone. Arthritis Rheum 2019;71(6):916–24.

[14] Suri S, Gill SE, Massena de Camin S, Wilson D, McWilliams DF, Walsh DA. Neurovascular invasion at the osteochondral junction and in osteophytes in osteoarthritis. Ann Rheum Dis 2007;66(11):1423–8.

[15] Damen J, Schiphof D, Wolde ST, Cats HA, Bierma-Zeinstra SM, Oei EH. Inter-observer reliability for radiographic assessment of early osteoarthritis features: the CHECK (cohort hip and cohort knee) study. Osteoarthritis Cartilage 2014;22(7): 969–74.

[16] Collins NJ, Misra D, Felson DT, Crossley KM, Roos EM. Measures of knee function: international knee documentation committee (IKDC) subjective knee evaluation form, knee injury and osteoarthritis outcome score (KOOS), knee injury and osteoarthritis outcome score physical function short form (KOOS-PS), knee outcome survey activities of daily living scale (KOS-adl), lysholm knee scoring scale, oxford knee score (OKS), western Ontario and McMaster Universities osteoarthritis index (WOMAC), activity rating scale (ARS), and tegner activity score (TAS). Arthritis Care Res 2011;63(Suppl 11):S208–28. 0 11.

[17] Guermazi A, Hayashi D, Roemer FW, Niu J, Yang M, Lynch JA, et al. Cyst-like lesions of the knee joint and their relation to incident knee pain and development of radiographic osteoarthritis: the MOST study. Osteoarthritis Cartilage 2010;18(11): 1386–92.

[18] Durnea CM, Siddiqi S, Nazarian D, Munneke G, Sedgwick PM, Doumouchtsis SK. 3D-Volume rendering of the pelvis with emphasis on paraurethral structures based on MRI scans and comparisons between 3D slicer and OsiriX. J Med Syst 2021; 45(3):27.

[19] Pritzker KP, Gay S, Jimenez SA, Ostergaard K, Pelletier JP, Revell PA, et al. Osteoarthritis cartilage histopathology: grading and staging. Osteoarthritis Cartilage 2006;14(1):13–29.

[20] Obeidat AM, Miller RE, Miller RJ, Malfait AM. The nociceptive innervation of the normal and osteoarthritic mouse knee. Osteoarthritis Cartilage 2019;27(11): 1669–79.

[21] Ikeuchi M, Wang Q, Izumi M, Tani T. Nociceptive sensory innervation of the posterior cruciate ligament in osteoarthritic knees. Arch Orthop Trauma Surg 2012; 132(6):891–5.

[22] Pivetta E, Scapolan M, Pecolo M, Wassermann B, Abu-Rumeileh I, Balestreri L, et al. MMP-13 stimulates osteoclast differentiation and activation in tumour breast bone metastases. Breast Cancer Res 2011;13(5):R105.

[23] Pelletier JP, Boileau C, Brunet J, Boily M, Lajeunesse D, Reboul P, et al. The inhibition of subchondral bone resorption in the early phase of experimental dog osteoarthritis by licofelone is associated with a reduction in the synthesis of MMP-13 and cathepsin K. Bone 2004;34(3):527–38.

[24] Mattap SM, Aitken D, Wills K, Laslett L, Ding C, Pelletier JP, et al. How do MRI-detected subchondral bone marrow lesions (BMLs) on two different MRI sequences correlate with clinically important outcomes? Calcif Tissue Int 2018;103(2): 131–43.

[25] Kornaat PR, Bloem JL, Ceulemans RY, Riyazi N, Rosendaal FR, Nelissen RG, et al. Osteoarthritis of the knee: association between clinical features and MR imaging findings. Radiology 2006;239(3):811–7.

[26] Torres L, Dunlop DD, Peterfy C, Guermazi A, Prasad P, Hayes KW, et al. The relationship between specific tissue lesions and pain severity in persons with knee osteoarthritis. Osteoarthritis Cartilage 2006;14(10):1033–40.

[27] Landells JW. The bone cysts of osteoarthritis. J Bone Joint Surg Br 1953;35-b(4): 643–9.

[28] Rhaney K, Lamb DW. The cysts of osteoarthritis of the hip; a radiological and pathological study. J Bone Joint Surg Br 1955;37-b(4):663–75.

[29] Carrino JA, Blum J, Parellada JA, Schweitzer ME, Morrison WB. MRI of bone marrow edema-like signal in the pathogenesis of subchondral cysts. Osteoarthritis Cartilage 2006;14(10):1081–5.

[30] Zanetti M, Bruder E, Romero J, Hodler J. Bone marrow edema pattern in osteoarthritic knees: correlation between MR imaging and histologic findings. Radiology 2000;215(3):835–40.

[31] Pouders C, De Maeseneer M, Van Roy P, Gielen J, Goossens A, Shahabpour M. Prevalence and MRI-anatomic correlation of bone cysts in osteoarthritic knees. AJR Am J Roentgenol 2008;190(1):17–21.

[32] Chen Y, Hu Y, Yu YE, Zhang X, Watts T, Zhou B, et al. Subchondral trabecular rod loss and plate thickening in the development of osteoarthritis. J Bone Miner Res 2018;33(2):316–27.

[33] He Z, Chu L, Liu X, Han X, Zhang K, Yan M, et al. Differences in subchondral trabecular bone microstructure and finite element analysis-based biomechanical properties between osteoporosis and osteoarthritis. J Orthop Translat 2020;24: 39–45.

[34] Boileau C, Tat SK, Pelletier JP, Cheng S, Martel-Pelletier J. Diacerein inhibits the synthesis of resorptive enzymes and reduces osteoclastic differentiation/survival in osteoarthritic subchondral bone: a possible mechanism for a protective effect against subchondral bone remodelling. Arthritis Res Ther 2008;10(3):R71.

[35] Mazur CM, Woo JJ, Yee CS, Fields AJ, Acevedo C, Bailey KN, et al. Osteocyte dysfunction promotes osteoarthritis through MMP13-dependent suppression of subchondral bone homeostasis. Bone Res 2019;7:34.

[36] Sabokbar A, Crawford R, Murray DW, Athanasou NA. Macrophage-osteoclast differentiation and bone resorption in osteoarthrotic subchondral acetabular cysts. Acta Orthop Scand 2000;71(3):255–61.

[37] Cattin AL, Burden JJ, Van Emmenis L, Mackenzie FE, Hoving JJ, Garcia Calavia N, et al. Macrophage-induced blood vessels guide schwann cell-mediated regeneration of peripheral nerves. Cell 2015;162(5):1127–39.

[38] Huang R, Wang X, Zhou Y, Xiao Y. RANKL-induced M1 macrophages are involved in bone formation. Bone Res 2017;5:17019.

[39] Weber A, Chan PMB, Wen C. Do immune cells lead the way in subchondral bone disturbance in osteoarthritis? Prog Biophys Mol Biol 2019;148:21–31.

[40] Pezet S, McMahon SB. Neurotrophins: mediators and modulators of pain. Annu Rev Neurosci 2006;29:507–38.

[41] Sanga P, Katz N, Polverejan E, Wang S, Kelly KM, Haeussler J, et al. Efficacy, safety, and tolerability of fulranumab, an anti-nerve growth factor antibody, in the treatment of patients with moderate to severe osteoarthritis pain. Pain 2013; 154(10):1910–9.

[42] Walsh DA, McWilliams DF, Turley MJ, Dixon MR, Fransès RE, Mapp PI, et al. Angiogenesis and nerve growth factor at the osteochondral junction in rheumatoid arthritis and osteoarthritis. Rheumatology 2010;49(10):1852–61.

[43] Xie H, Cui Z, Wang L, Xia Z, Hu Y, Xian L, et al. PDGF-BB secreted by preosteoclasts induces angiogenesis during coupling with osteogenesis. Nat Med 2014;20(11): 1270–8.

[44] Mapp PI, Walsh DA. Mechanisms and targets of angiogenesis and nerve growth in osteoarthritis. Nat Rev Rheumatol 2012;8(7):390–8.

[45] Burr DB, Gallant MA. Bone remodelling in osteoarthritis. Nat Rev Rheumatol 2012; 8(11):665–73.

[46] Stapledon CJM, Tsangari H, Solomon LB, Campbell DG, Hurtado P, Krishnan R, et al. Human osteocyte expression of Nerve Growth Factor: the effect of Pentosan Polysulphate Sodium (PPS) and implications for pain associated with knee osteoarthritis. PLoS One 2019;14(9):e0222602.

[47] Scanzello CR, Goldring SR. The role of synovitis in osteoarthritis pathogenesis. Bone 2012;51(2):249–57.